Med Chem Res
DOI 10.1007/s00044-015-1346-4

ORIGINAL RESEARCH

Discovery of Rimonabant and its potential analogues as anti-TB drug candidates

J. M. Gajbhiye · N. A. More · Manoj D. Patil · R. Ummanni · S. S. Kotapalli · P. Yogeeswari · D. Sriram · V. H. Masand

Received: 25 September 2014 / Accepted: 19 February 2015

Abstract Rimonabant and its analogues have been synthesized in moderate to good yields using a simple synthetic route. All the newly synthesized compounds were subjected to in vitro screening against *M. tuberculosis* and *M. smegmatis*. The most potent analogue JMG-14 exhibits MIC value of 3.13 compared to 3.25 and 50 μg/ml for ethambutol and pyrazinamide, respectively. The molecular docking reveals that pyrazole ring, number and position of halogen atoms play a crucial role in deciding interactions with MTCYP-121. These findings open up a new avenue in the search of potent anti-TB drugs with rimonabant and its novel analogue JMG-14 as lead molecules.

Graphical Abstract

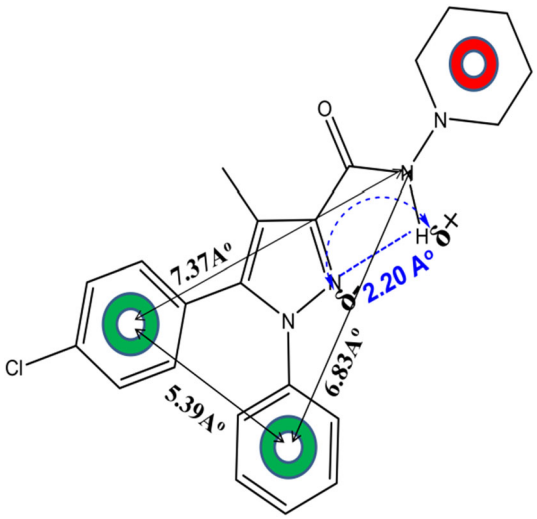

Keywords Rimonabant · Diaryl pyrazoles · Tuberculosis · Mycobacterium tuberculosis · H37Rv · MTCYP-121

J. M. Gajbhiye (✉) · N. A. More · M. D. Patil
Division of Organic Chemistry, CSIR-National Chemical Laboratory, Pune 411008, India
e-mail: jm.gajbhiye@ncl.res.in

R. Ummanni · S. S. Kotapalli
Centre for Chemical Biology, Indian Institute of Chemical Technology, Hyderabad 500607, India

P. Yogeeswari · D. Sriram
Tuberculosis Drug Discovery Laboratory, Pharmacy Group, Birla Institute of Technology and Science, Pilani, Hyderabad Campus, Hyderabad 500078, India

V. H. Masand
Department of Chemistry, VidyaBharati College, Camp, Amravati 444602, India

Introduction

Tuberculosis (TB) is among the deadly diseases afflicting mankind, and it still remains a major public health burden in many developing countries (Corbett *et al*., 2003). Approximately one-third of the world's population is still under the ill influence of TB. In 2011, nearly 9 million people around the world suffered from TB (WHO 2013), with 1.4 million deaths worldwide. Recent reports reveal that every year 0.2 million from 0.7 million HIV patients die due to TB,

Published online: 07 March 2015

and thus, TB is a leading killer in HIV-infected patients (Nunn *et al*., 2005; Masand *et al*., 2012; Shukla *et al*., 2014). Emerging resistance to the marketed anti-tuberculosis drugs is a major concern that threatens progress made in TB care and control worldwide (Shukla *et al*., 2014). In most of the cases, drug resistance (Chiang and Schaaf, 2010) arises due to the improper use of antibiotics in chemotherapy, administration of improper treatment regimens and failure to ensure that patient completes the whole course of the treatment (Elzinga *et al*., 2004; Kumar *et al*., 2013). To combat the continuous rise in multidrug-resistant TB, scientific efforts are concentrated on inventing new agents for the treatment of TB. Despite the efforts executed in laboratories and hospitals, TB is nevertheless a major challenge to medicinal chemists.

Developing a new drug is a long, expensive and tedious process, often consuming several years and resources. In addition, the regulatory approval process following the drug discovery/design involves several tests and trials. Even after completing the whole process of drug development, certain drugs such as celecoxib, sibutramine, rimonabant, though approved by the regulatory agencies, were withdrawn from the market due to the appearance of the side effects. At the current stage, it would be a highly beneficial and attractive strategy to identify a drug candidate, which has been approved as a drug by regulatory authorities, effective for the treatment of TB. This would enable a quicker introduction of the drug into the market for TB treatment. In the recent years, azoles viz. pyrazoles, imidazoles and triazoles have attracted the attention of researchers. Some clinically used drugs such as clotrimazole, fluconazole and voriconazole, which contain azole moiety, can be used to treat generalized systemic mycoses. Literature survey reveals that selected azole drugs possess potent anti-mycobacterial activity in the nanomolar range (Kumar *et al*., 2013; Menozzi *et al*., 2004) (Fig. 1).

It has been established (McLean *et al*., 2002; Hudson *et al*., 2012) that many azole compounds possessing potent anti-tubercular activity bind to MT-CYP51 and MT-CYP121, proteins with crucial role in metabolism of *M. tuberculosis*, possessing high affinity and retard the growth of *Mycobacterium bovis* and *Mycobacterium smegmatis*, the two mycobacterial species which closely resemble *M. tuberculosis*. In recent years, cytochrome P450 (CYP121) has gained popularity as an attractive target for designing potent azole-based drugs against *M. tuberculosis*, a plausible reason is that MT-CYP121, which has unique catalytic action, binds commercially available azole drugs with a higher affinity than MT-CYP51 (Menozzi *et al*., 2004). In addition, it has no equivalent enzyme in humans. MT-CYP121 is necessary for bacterial viability since it catalyzes an unusual intramolecular carbon–carbon coupling reaction (Dumas *et al*., 2013). The high affinity of the azole derivatives such as

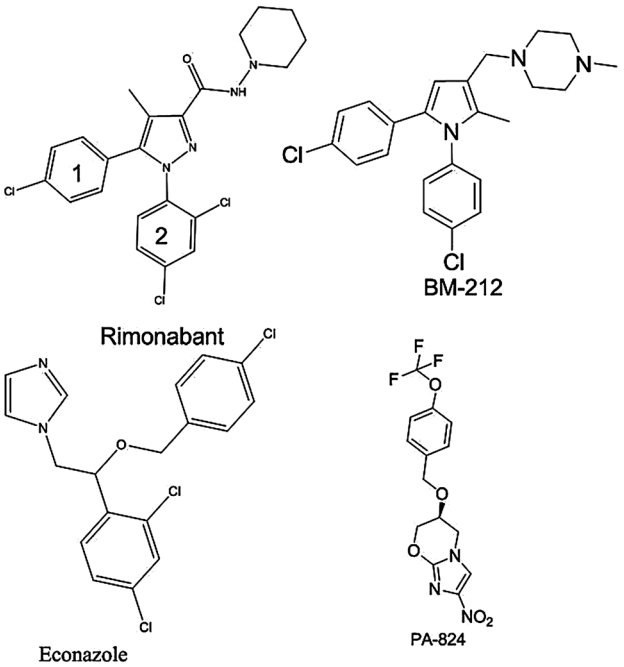

Fig. 1 Azole and pyrazole derivatives possessing anti-tubercular activity

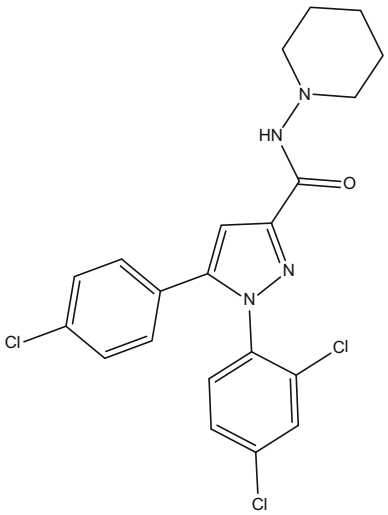

Fig. 2 2D-structure of rimonabant

clotrimazole for MT-CYP121 is attributed to their bulky, polycyclic structure, enhancing favorable interactions with the hydrophobic residues in the largely non-polar active site of the enzyme. Moreover, in many studies, the presence of halogen attached to aromatic moiety has been found to escalate antifungal and anti-mycobacterial activities (Dumas *et al*., 2013; Sundaramurthi *et al*., 2011; Belin *et al*., 2009). Rimonabant (**1**) (Fig. 2), a pyrazole carboxylic acid derivative discovered by Sanofi-Synthelabo in 1994 as the first potent, orally active, selective CB_1 cannabinoid receptor antagonist and sold under several trade names as an anorectic

anti-obesity drug. Rimonabant and its analogues were also shown to have promising activities and also proved safe to human (Lange and Kruse, 2005). It was recently withdrawn (Kang and Park, 2012) from the market following post-marketing surveillance studies, which confirmed a risk of depressive disorders among users. However, modification or elimination of the side chain attached to carboxamide (Jagerovic *et al*., 2008) which is responsible for crossing the blood–brain barrier might reduce the side effects. There are several important anti-TB drug candidates such as PA-824 and BM212, which are structurally reminiscent to rimonabant **1**, and hence, we were curious to study its anti-TB properties. All these observations prompted us to develop new rimonabant analogues that may prove effective against multidrug-resistant strains of the tuberculosis pathogen.

Chemistry

The synthesis of compounds **2**, **3**, **7**, **8**, **9**, **11**, **12**, and **13** was carried out as outlined in the Scheme 1. 4-Chloropropiophenone (A) on condensation with diethyl oxalate in the presence of LiHMDS gave lithium salt of ethyl 4-(4-chlorophenyl)-3-methyl-4-oxydo-2-oxobuten-3-oate (B). This on condensing with 2, 4-dichlorophenyl hydrazine hydrochloride and phenyl hydrazine hydrochloride in ethanol gave hydrazones, which on refluxing in acetic acid for 24 h yielded esters **3** and **8**, respectively. Subsequent reaction of B with suitable hydrazines in 50 % sulfuric acid and ethanol at 79 °C for 14 h yielded desired acids (**2**, **7**, **9**, **11**, **12** and **13**). These acids on subsequent treatment with thionyl chloride afforded acid chlorides. Finally, the amidation was executed to afford the target compounds **1**, **4**, **5**, **6**, **10**, **14**, **15**, **16**, **17**, **18** and **19** in moderate to good yields (Schemes 2, 3, 4). The structures of newly synthesized compounds were established on the basis of spectral and physicochemical analyses.

Results and discussion

Our initial study involved screening of rimonabant **1** against *M. smegmatis*. Interestingly, it exhibited a MIC value of 13.56 compared to 16 μg/ml for isoniazid. Therefore, its 18 analogues were synthesized (Lan *et al*., 1999; Kotagiri *et al*., 2007), and few of them were screened against *M. smegmatis*. They showed moderate to high activity (Table 1). Encouraged by the results, rimonabant and all the synthesized analogues were then screened for *Mycobacterium tuberculosis* (virulent strain H37Rv) in vitro (Moore *et al*., 1999). The details of the screening data are shown in Table 1.

The precursor of rimonabant acid **2** showed improved MTB activity and ester 3 retains the activity as compared to rimonabant. Similarly, the analogues **2**, **4**, **7**, **11** and **15**–**18** exhibited enhanced activity, and the analogues **3**, **5**, **6**, **8**, **10**, **12** & **19** were also found to be active. Most importantly, the analogues **9** and **13** showed very good MTB activity. The analogue JMG-14 came out to be a promising lead with highest activity. Compared with one of the first-line anti-TB drug ethambutol (MIC 3.25 μg/ml), the analogue JMG-14 was found to be equally active. When compared to pyrazinamide (MIC 50.0 μg/ml), all the **18** analogues were found to be more potent. The analogue **13** also emerged as another lead molecule, which can be explored further.

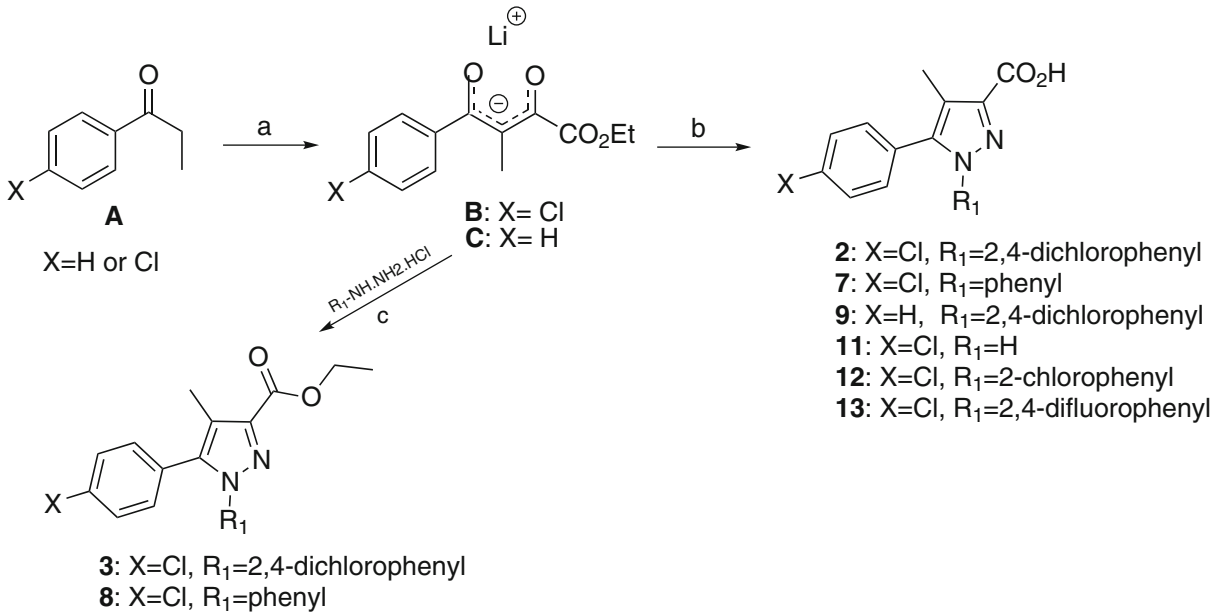

Scheme 1 Reagents and conditions: (a) LiHMDS, diethyl oxalate, methyl cyclohexane, 15–25 °C, 6th; (b) R_1-NH-NH_2·HCl, 50 % aq. H_2SO_4, EtOH, 79 °C, 14th; (c) EtOH, rt, 20 h, then AcOH, reflux, 24 h

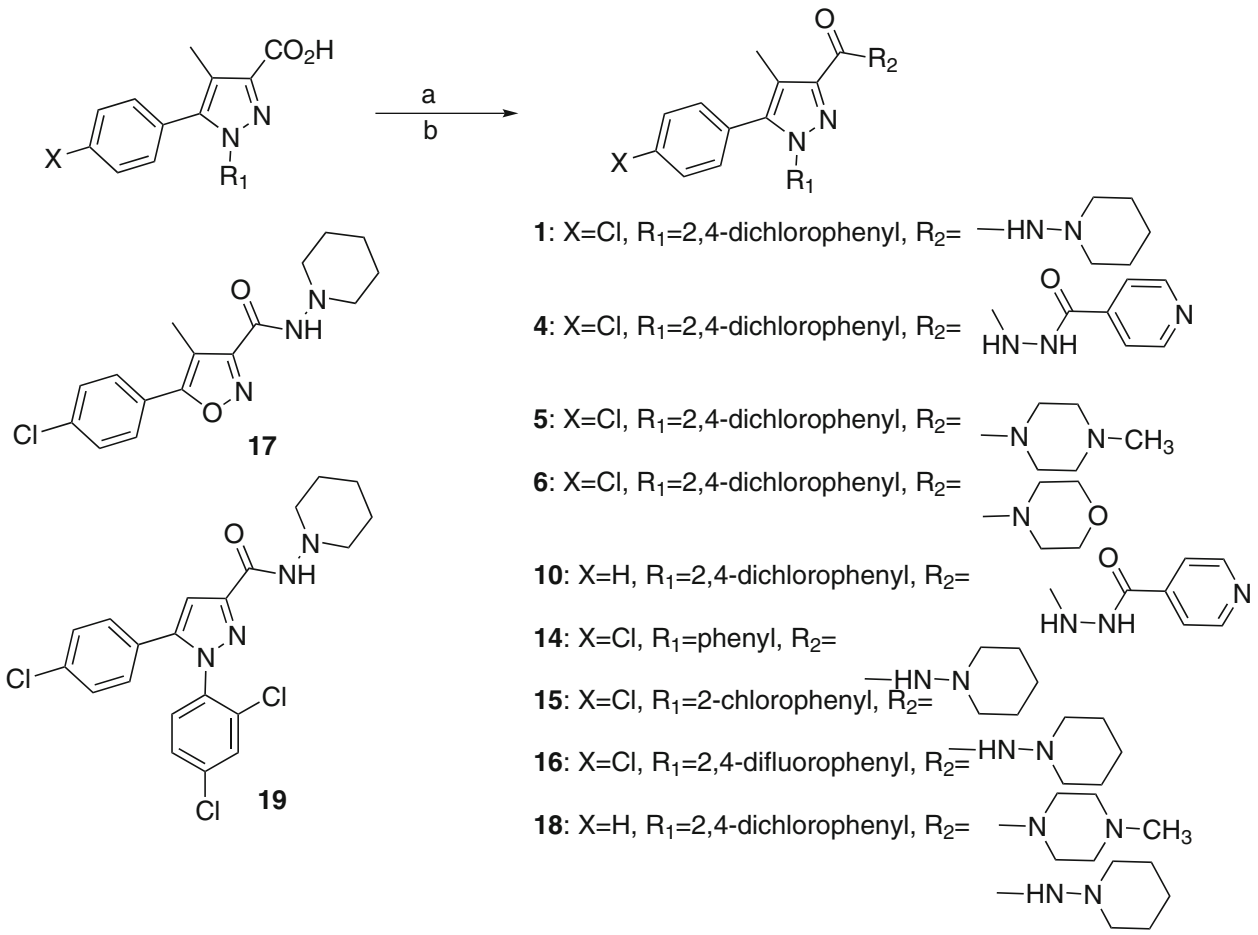

Scheme 2 Reagents and conditions: (a) thionyl chloride. DMF (cat.) toluene. 100 °C, 4 h (b) Et_3N sutiable amide. 0°-rt. 12 h

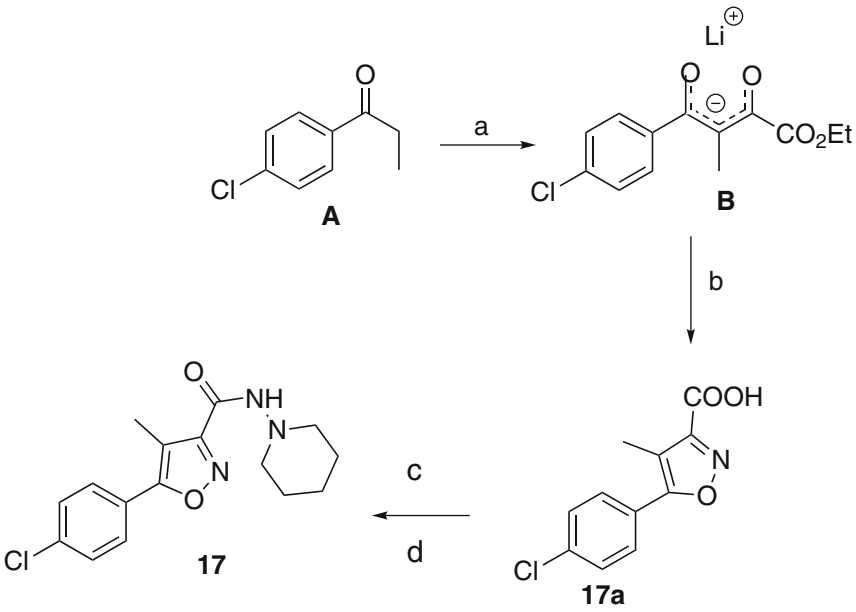

Scheme 3 Reagents and conditions: (a) LiHMDS, diethyl oxalate, methyl cyclohexane, 15–25 °C, 6h; (b) $NH_2OH{\cdot}HCl$, 50% aq. H_2SO_4, EtOH, 79 °C, 14h; (c) thionyl chloride, DMF (cat), toluene, 100 °C, 4th; (d) Et_3N, 1-aminopiperidine, 0°-rt, 12 h

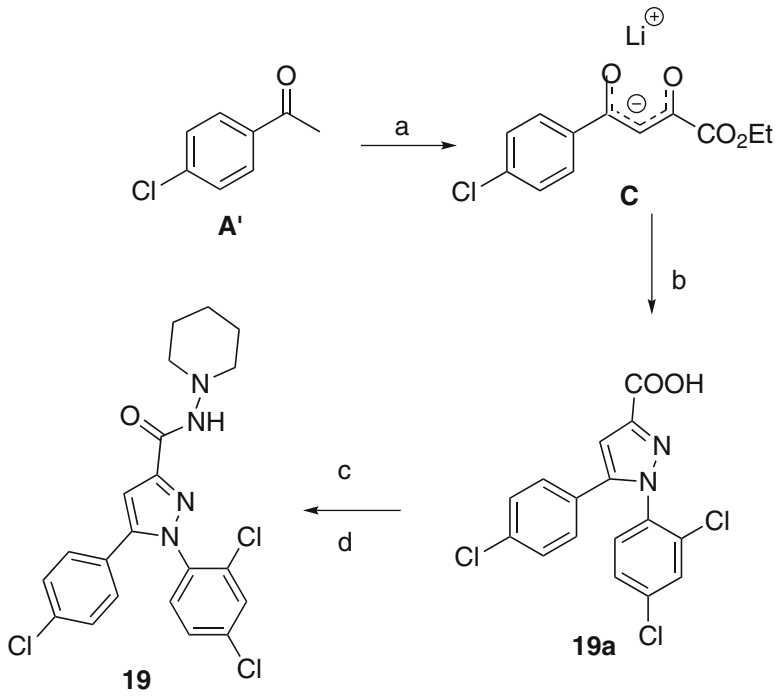

Scheme 4 Reagents and conditions: (a) LiHMDS, diethyl oxalate, methyl cyclohexane, 15–25 °C, 6h; (b) 2,4-dichlorophenylhydrazine. HCl, 50% aq. H_2SO_4, EtOH, 79 °C, 14 h; (c) thionyl chloride, DMF (cat), toluene, 100 °C, 4 h; (d) Et_3N, 1-aminopiperidine, 0°-rt, 12 h

Table 1 In vitro anti-mycobacterial activity of rimonabant (**1**) and synthesized analogues

S. No.	CLog*P*[b]	% inhibition *M. Smegmatis*	MIC (μg/ml) M. TB[a]	S. No.	CLog*P*[b]	% inhibition *M. Smegmatis*	MIC (μg/ml) M. TB
1	6.471	99.33 MIC 13.56 μg/ml	25	13	4.981	NT	6.25
2	6.121	22.84	12.5	14	5.031	99.70	3.13
3	7.083	14.07	25	15	5.754	NT	12.5
4	5.532	19.21	12.5	16	4.526	NT	12.5
5	5.666	14.50	25	17	3.342	NT	12.5
6	5.335	NT	>25	18	5.756	32.37	12.5
7	4.681	17.70	12.5	19	6.841	NT	25
8	5.234	22.70	25	Isoniazid		16 μg/ml	0.05
9	5.407	15.73	6.25	Rifampicin		2 μg/ml	0.1
10	4.818	1.362	25	Ethambutol		NT	3.25
11	3.035	NT	12.5	Pyrazinamide		NT	50.0
12	5.404	NT	25				

NT not tested

[a] *Mycobacterium tuberculosis* H37Rv

[b] Calculated LogP using ChemDraw 12

Based on the analogue **9**, a simple replacement of chlorine by hydrogen might provide a more active analogue of **13**.

The main purpose of this study was to introduce modification on the side chain on carboxamide moiety of rimonabant and its analogues to develop new potential anti-TB agents. In the present work, diverse functional groups were introduced on the side chain of the carboxamide moiety of rimonabant to identify structure–activity relationships. It appears that the piperidinyl side chain is not must for high activity and derivatives with free acids are better candidates for further evaluation. Variation of phenyl ring attached to nitrogen (of pyrazole moiety) shows prominent effect on the activity, and this observation is further vindicated by the docking analysis. The substitution on the ring or its complete removal as well as replacement of that nitrogen with oxygen shows positive effect. Alteration on the *p*-chlorophenyl ring present on central pyrazole also influences the bioactivity. The methyl group seems to be important for the activity, since the analogue without methyl shows diminished activity.

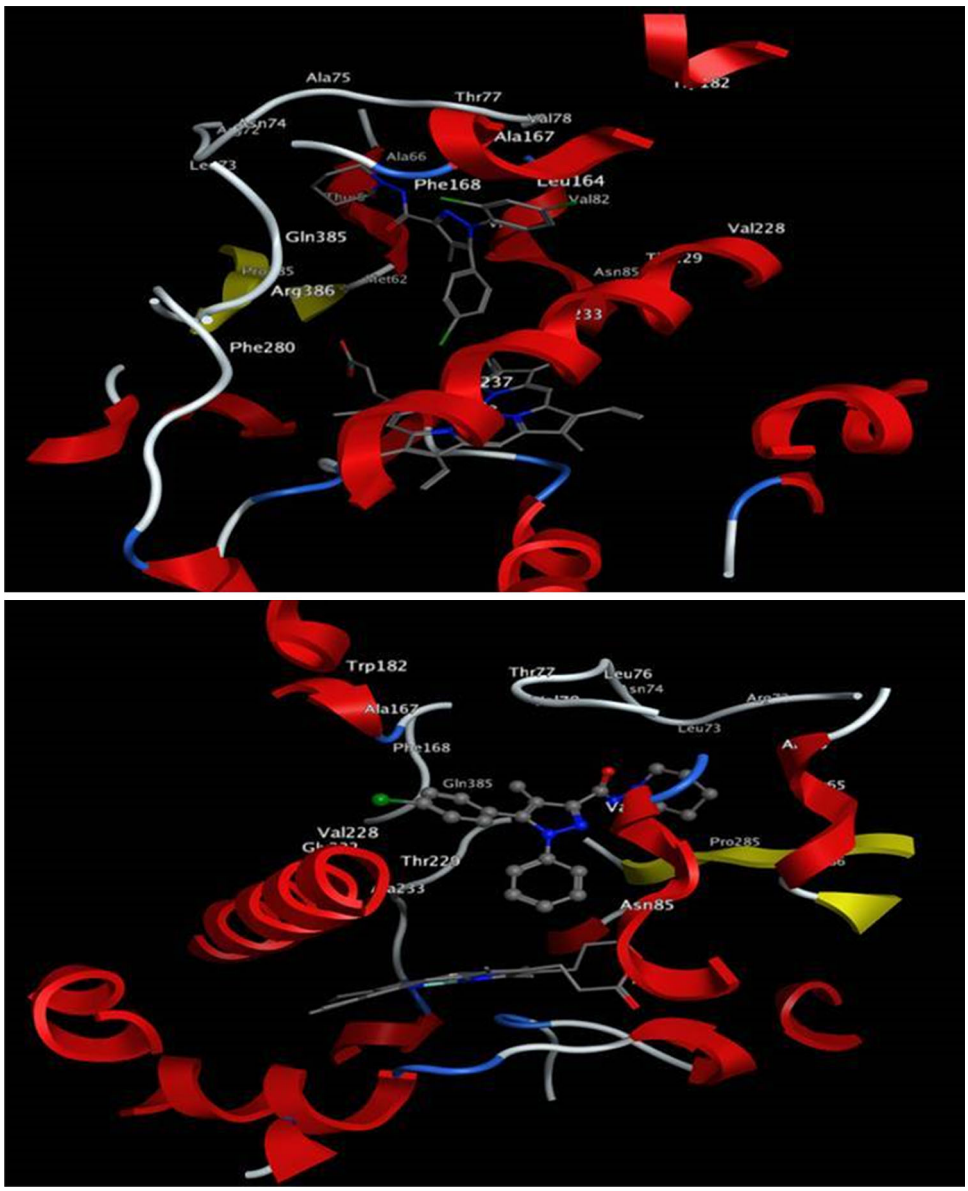

Fig. 3 Docking pose for **a** rimonabant (compound **1**) and **b** most active compound **14**

Docking analysis

Molecular docking analysis was performed to determine the structural features that steer the biological profile of Rimonabant and its novel analogues. As stated earlier (Dumas *et al*., 2013; Sundaramurthi *et al*., 2011; Belin *et al*., 2009), the mechanism of action for anti-TB activity involves interaction of pyrazoles with MTCYP-121; therefore, molecular docking analysis was performed to determine the structural features that govern the anti-TB of present series molecules. The docking analysis was performed for all the compounds, but for the sake of convenience, we represent the docking poses for compounds **1** and **14** as representatives. The active site of MT-CYP121, a heme-based enzyme that transfers a single oxygen atom to the substrate, comprises of Thr-77, Val-82, Val-83, Asn-85, Met-86, Ala-167, Ph-168, Thr-229, Ala-233, Ser-237, Gln-385 and Arg-386. The catalytic site is located on top of the distal side of the heme, where oxygen binds, near to I-helix (Dumas *et al*., 2013; Sundaramurthi *et al*., 2011; Belin *et al*., 2009).

According to the results of our docking experiments (see Fig. 3), the prominent interactions between compound **1** and the receptor are van der Waals, H-bonding and hydrophobic in nature. The compound **1** could adopt bent 'T' shape (or weird propeller shape) while interacting with the cytochrome catalytic site (1350 $Å^3$ in size) orienting chloro atom attached to benzene ring 1 toward the iron atom of the heme group with the heterocyclic rings (pyrazole and piperidine) pointing toward polar residues. Binding of compound **1** involves numerous van der Waals contacts

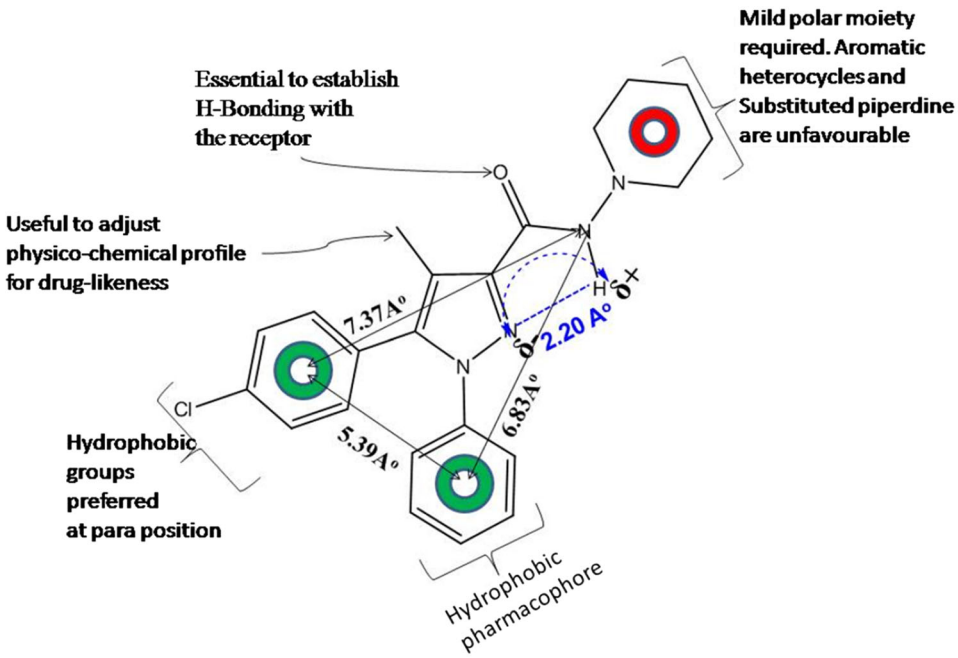

Fig. 4 Summary of SAR and molecular docking analysis for anti-TB activity of rimonabant and its analogues

with the hydrophobic side chains of Leu-76, Val-78, Val-83, Ala-167 and Phe-168. There are water-mediated H-bond network with the N (non-substituted) of pyrazole ring and with N (amide group). Furthermore, a strong H-bond between Arg-72 with N (piperidine ring) enhances the anchoring of compound **1** with CYP-121. The presence of pyrazole moiety in close proximity to Gln-385 indicates that it plays a crucial role in inhibiting the normal functioning of CYP-121.

Compound **14**, like compound **1**, adopts bent 'T' shape while interacting with CYP-121, but interacts with more number of residues of the active site than the compound **1**. The ring 2 is closer to heme moiety with ring 1 pointing toward hydrophobic residues Val-78, Phe-168, Trp- 182 and Val-228. Another remarkable difference in interaction pattern of compounds **1** and **14** is due to the involvement of one and two water molecules, respectively, in enhancing the polar interactions with the receptor. The binding between the receptor and the substrate is enhanced by the water-mediated H-bonding between Thr-77 and the oxygen atom of amide group as well between Arg-72 and N (piperidine moiety).

A plausible reason for bent 'T' shape for compounds **1** and **14** is the presence of bulky Ser-237 in close proximity to phenyl ring attached to N of pyrazole moiety. Another reason could be the presence of unusually close other I-helix residues above the heme. Compounds **1** and **14** have adopted exactly opposite conformations while interacting with the receptor, and this could be attributed to the steric repulsion exerted by bulkier -Cl atoms present as substituents on the phenyl ring. Hudson *et al*. recently reported that the azoles do not coordinate with the heme iron, as is typically observed for the azole antifungal CYP inhibitors (Hudson *et al*., 2012). Our docking experiment also concurs with this. The N (δ−)/N–H (δ+) with a distance of 2.20 Å (depicted in Fig. 3), acting as polar pharmacophore, are responsible for establishing the polar contacts with the receptor.

The molecular docking and structure–activity relationships (SAR) have been summarized in Fig. 4.

Further studies being carried out in our laboratory to explore the mechanism of action of this scaffold and evaluation of these compounds for anti-bactericidal activity as well as activity under alternate growth conditions such as non-replicating growth conditions.

Pharmacology

Anti-mycobacterial activity assay

Anti-mycobacterial activity of the synthesized compounds was performed against *Mycobacterium smegmatis* MC2155 strain using growth inhibition assay by agar dilution followed by turbidimetry method. The assay was semi-throughput and conducted in a 96-well plate (sterile). For *M. tuberculosis*, H37Rv strain was utilized by performing a growth inhibition assay from fresh Middlebrook 7H11 agar slants. This method is similar to that recommended by the National Committee for Clinical Laboratory Standards (NCCLS, 1995) for the determination of minimum inhibitory concentration (MIC) in duplicate.

Conclusion

For the first time, it has been shown that rimonabant could be a lead molecule for finding more potent anti-TB drug candidates. In the present work, JMG-14 is the most potent analogue of rimonabant, emerging as a suitable lead molecule, which can be further optimized using the SAR and molecular docking analyses. Currently, research work is in progress on the development of more rational analogues and their anti-TB.

Experimental

Chemistry

All the reagents and the solvents were used as received from commercial sources unless and otherwise stated. All the experiments were carried out under an atmosphere of nitrogen in round-bottom flask. Pre-coated plates (silica gel 60 PF254, 0.25 mm or 0.5 mm) were utilized for thin-layer chromatography (TLC). Column chromatographic purifications were carried out on flash silica gel (100–200 mesh) using either petroleum ether and ethyl acetate or dichloromethane and methanol as eluents. Melting points (mp) are uncorrected and were measured on an electrothermal melting point apparatus. The IR spectra were recorded on an FT-IR spectrometer. The ^{1}H and ^{13}C NMR spectra were recorded on 200/400/500 MHz and 50/100/125 MHz NMR spectrometer, respectively, in $CDCl_3$/DMSO-d_6. Mass spectra were taken on LC–MS (ESI) mass spectrometer. HRMS were scanned at NCL, Pune.

Preparation of Lithium salt of Ethyl 4-(4-chlorophenyl)-3-methyl-4-oxydo-2-oxobuten-3-oate (**B**) Methylcyclohexane (30 ml) and lithium hexamethyldisilazane (30 ml, 31.7 mmol) were introduced in a round-bottom flask under nitrogen atmosphere and cooled to 15–25 °C. A solution of 4-chloropropiophenone (A, 5.0 g, 29.65 mmol) in methylcyclohexane (12.5 ml) was slowly added with continuous stirring for 2.5 h. To this reaction mixture, diethyl oxalate (4.78 g, 32.6 mmol) was added with stirring. The reaction progress was monitored by TLC; the solid obtained was filtered, washed with methylcyclohexane (30 ml) and dried under vacuum (30 min) to afford the lithium salt (Kotagiri *et al*., 2007) (Cream yellow solid, 5.7 g, 71.9 %).

Preparation of ethyl 5-(4-Chlorophenyl)-1-(2,4-dichlorophenyl)-4-methyl-1H-pyrazole-3-carboxylate (**3**) To a continuously stirring solution of lithium salt B (1.0 g, 3.64 mmol) in 15 ml of ethanol was added 2,4-dichlorophenyl hydrazine hydrochloride (0.777 g, 3.64 mmol) at room temperature. The shaking was carried for 20 h till precipitate was obtained. The precipitate so obtained was filtered and washed with ethanol (10 ml) and dried under vacuum to give a pale yellow solid (1.1 g), which was dissolved in acetic acid (10 ml) and refluxed for 24 h. On completion of the reaction (TLC), the reaction mixture was poured into cold water (20 ml) and then extracted with ethyl acetate (3 × 15 ml). The combined extracts were washed with water, saturated sodium bicarbonate solution, brine and then dried under vacuum to give the crude product. It was then purified by column chromatography on silica gel using ethyl acetate/petroleum ether (1:9) as elution system to give the ester 3 (Kotagiri *et al*., 2007), (670 mg, 45 %,) pale yellow solid.mp 128–129 °C;^{1}H NMR ($CDCl_3$, 200 MHz): δ 7.39 (d, $J = 2.02$ Hz, 1H), 7.34 (d, $J = 1.37$ Hz, 1H), 7.33–7.28 (m, 3H), 7.08 (d, $J = 8.59$ Hz, 2H), 4.51–4.41 (q, $J = 7.08$ Hz, 2H), 2.34 (s, 3H), 1.43 (t, $J = 7.08$ Hz, 3H); ^{13}C NMR ($CDCl_3$, 100 MHz): δ 162.7, 142.9, 136.0, 135.9, 135.0, 133.0, 130.9, 130.7, 130.1, 128.9, 127.7, 127.0, 119.1, 60.9, 14.4, and 9.6.HRMS-ESI (m/z) Calcd. $C_{19}H_{15}O_2N_2Cl_3$ + H)+: 409.0272 found: 409.0265.

Preparation of 1-(5-(4-Chlorophenyl)-4-methyl-1-phenyl-1H-pyrazol-3-yl)propan-1-one (**8**) Synthesis of **8** was accomplished according to the procedure applied for **3**. Pale orange solid; 595 mg, 48 %; mp 121–123 °C; ^{1}H NMR ($CDCl_3$, 400 MHz): δ 7.31–7.36 (m, 5H), 7.24–7.27 (m, 2H), 7.10 (d, $J = 8.6$ Hz, 2H), 4.48 (q, $J = 14.14$ Hz, 2H), 2.33 (s, 3H), 1.46 (t, $J = 7.07$ Hz, 3H); ^{13}C NMR ($CDCl_3$, 100 MHz): δ 163.0, 142.3, 140.9, 139.3, 134.7, 131.3, 128.9, 128.0, 127.9, 127.0, 125.4, 120.0, 60.8, 14.4, 9.7; HRMS-ESI (m/z) Calcd. $C_{19}H_{17}O_2N_2ClNa$: 363.0871 found: 363.0868.

Preparation of 5-(4-Chlorophenyl)-1-(2,4-dichlorophenyl)-4-methyl-1H-pyrazole-3-carboxylic acid (**2**) A mixture of lithium salt of ethyl 4-(4-chlorophenyl)-3-methyl-4-oxydo-2-oxobuten-3-oate (B, 1.0 g, 3.6 mmol), ethanol (25 ml), 2,4-dichlorophenyl hydrazine hydrochloride (0.777 g, 3.6 mmol), and 50 % sulfuric acid (10 ml) was refluxed for 6 h. After the reaction was complete (TLC), ethanol was removed under reduced pressure, and again, a second installment of 50 % sulfuric acid (20 ml) was added, followed by refluxing for 8 h. The reaction mixture was cooled to room temperature (35 °C) and was poured onto crushed ice, stirred for 15 min, filtered and washed with water (20 ml). The wet solid so obtained was stirred with water (30 ml), and the pH was adjusted to >10 with 20 % dil. NaOH. This aqueous layer was washed with petroleum ether. The aqueous layer was separated, cooled to 0 °C, and pH was adjusted to 2.0 by concentrated hydrochloric acid. Solid so obtained was filtered, washed with water (100 ml) and dried to afford 2 (Kotagiri *et al*., 2007), (0.923 mg, 65 %), Off white solid, mp 208–209 °C; ^{1}H NMR ($CDCl_3$,

400 MHz): δ 7.44–7.41 (m, 1H), 7.35 (d, $J = 1.89$ Hz, 1H), 7.33–7.28 (m, 3H), 7.09 (d, $J = 8.47$ Hz, 2H), 2.36 (s, 3H); ^{13}C NMR ($CDCl_3$, 100 MHz): δ 166.4, 143.3, 136.2, 135.6, 135.1, 133.5, 130.8, 130.5, 129.8, 128.9, 127.8, 127.7, 126.7, 119.6, 9.6; HRMS-ESI (m/z) Calcd. $C_{17}H_{11}O_2N_2Cl_3Na$: 402.9778 found: 402.9781.

Preparation of 5-(4-Chlorophenyl)-4-methyl-1-phenyl-1H-pyrazole-3-carboxylic acid (**7**) Compound **7** was synthesized by the procedure applied for **2**. Pale brown solid: 719 mg, 58 %; mp 203–204 °C; ^{1}H NMR ($CDCl_3$, 200 MHz): δ 7.46 (s, 1H), 7.32–7.38 (m, 5H), 7.30–7.20 (m, 2H), 7.13 (d, $J = 6.36$ Hz, 2H), 2.35 (s,3H); ^{13}C NMR ($CDCl_3$, 400 MHz): δ 165.9, 141.3, 140.9, 139.0, 134.9, 131.3, 129.0, 128.2, 127.6, 125.4, 125.1, 120.5, 9.6; HRMS-ESI (m/z) Calcd. $C_{17}H_{13}O_2N_2ClNa$: 335.0571 found: 335.0566.

Preparation of 1-(2,4-dichlorophenyl)-4-methyl-5-phenyl-1H-pyrazole-3-carboxylic acid (**9**) Compound **9** was synthesized by the procedure applied to **2**. Cream solid: 865 mg, 59 %; mp 188–189 °C; ^{1}H NMR ($CDCl_3$, 400 MHz): δ 7.46 (s, 1H), 7.16–7.27 (m, 5H), 7.08 (s, 2H), 6.02 (s, 1H), 2.17 (s, 3H); ^{13}C NMR ($CDCl_3$, 100 MHz): δ 167.2, 145.6, 136.0, 135.1, 132.2, 131.2, 130.8, 129.6, 129.1, 128.5, 128.3, 128.2, 127.8, 118.0, 9.7; HRMS-ESI (m/z) Calcd. $C_{17}H_{12}O_2N_2Cl_2Na$: 369.0168 found: 369.0164.

Preparation of 5-(4-chlorophenyl)-4-methyl-1H-pyrazole-3-carboxylic acid (**11**) Compound **11** was synthesized by the procedure applied to **2**. Cream solid; 387 mg, 45 %; mp 288–290 °C; ^{1}H NMR (DMSO-d_6, 500 MHz): δ 13.54 (s, 1H), 7.89, (d, $J = 8.24$ Hz, 2H), 7.77 (d, $J = 8.24$ Hz, 2H), 2.61 (s, 3H); ^{13}C NMR (DMSO-d_6, 125 MHz): δ 162.4, 132.7, 130.9, 129.4, 128.9, 128.5, 117.0, 60.5, 9.9; HRMS-ESI (m/z) Calcd. $C_{11}H_9O_2N_2ClNa$: 259.0245 found: 259.0243.

Preparation of 1-(2-chlorophenyl)-5-(4-chlorophenyl)-4-methyl-1H-pyrazole-3-carboxylic acid (**12**) Compound **12** was synthesized by the procedure applied to **2**. Pale yellow solid: 656 mg, 52 %; mp 204–206 °C; ^{1}H NMR ($CDCl_3$, 200 MHz): δ 7.33–7.42 (m, 4H), 7.26 (d, $J = 6.41$ Hz, 2H), 7.04 (d, $J = 7.79$ Hz, 2 H), 2.32 (s, 3H);^{13}C NMR ($CDCl_3$, 100 MHz): δ 165.6, 143.3, 141.7, 136.9, 134.9, 131.9, 130.9, 130.3, 130.0, 129.8, 128.8 127.5, 126.9, 119.4, 9.6; HRMS-ESI (m/z) Calcd. $C_{17}H_{12}O_2N_2Cl_2Na$: 369.0168 found: 369.0168.

Preparation of 5-(4-chlorophenyl)-1-(2,4-difluorophenyl)-4-methyl-1H-pyrazole-3-carboxylic acid (**13**) Compound **13** was synthesized by the procedure applied to **2**. Pale brown solid; 781 mg, 62 %; mp 196–198 °C; ^{1}H NMR ($CDCl_3$, 500 MHz): δ 9.31 (bs, 1H), 7.44 (s, 1H), 7.27 (d, $J = 8.46$ Hz, 2H), 7.03 (d, $J = 8.46$ Hz, 2H), 6.87 (s, 1H), 6.72 (s, 1H), 2.25 (s, 3H); ^{13}C NMR ($CDCl_3$, 125 MHz): δ 161.7, 157.5, 155.5, 143.1, 135.0, 130.7, 130.0, 128.9, 127.0, 123.7, 119.5, 112.1, 111.9, 104.8, 9.6; HRMS-ESI (m/z) Calcd. $C_{17}H_{11}O_2N_2ClF_2Na$: 371.0369 found: 371.0369.

Procedure for the synthesis of 5-(4-Chlorophenyl)-1-(2,4-dichlorophenyl)-4-methyl-N-(piperidin-1-yl)-1H-pyrazole-3-carboxamide **1** To a stirred solution of 2 (382 mg; 1.0 mmol) in toluene (10 ml), one drop of dimethyl formamide was added. The reaction mixture was cooled to 0 °C and thionyl chloride (140 mg: 1.2 mmol) in 2 ml toluene was added dropwise for the period of 2 min at the same temperature. The reaction mixture was allowed to attain room temperature and heated at 100 °C for 4 h. Excess of thionyl chloride and toluene was distilled off under reduced pressure. In another flask under nitrogen atmosphere was introduced 1-aminopiperidine (100 mg; 1.0 mmol) and triethyl amine (101 mg; 1.0 mmol) in 5.0 ml dichloromethane. The flask was cooled to 0 °C. To this was added a cooled solution of acid chloride dropwise at the same temperature. The resulting reaction mixture was allowed to attain room temperature, and then, it was stirred for 12 h. After completion of the reaction (monitored by TLC), the reaction mixture was diluted with water (10 ml) and organic layer was separated, washed with water (2 × 5 ml) and brine solution (5 ml), dried over Na_2SO_4 and concentrated *in vacuo*. The residue was purified by column chromatography over silica gel (ethyl acetate/petroleum ether 1:9 (v/v)) afforded pure product.

White solid: 292 mg, 63 %; mp 182–183 °C;^{1}H NMR ($CDCl_3$, 400 MHz): δ 7.63 (s,1H), 7.41–7.36 (m, 1H), 7.30–7.26 (m, 3H), 7.04 (d, $J = 8.28$ Hz, 2H), 2.93–2.78 (m, 4H), 2.35 (s, 3H), 1.78–1.70 (m, 4H), 1.48–1.37 (m, 2H);^{13}C NMR ($CDCl_3$, 100 MHz): δ 159.9, 144.4, 142.9, 136.0, 135.9, 134.9, 132.9, 130.8, 130.6, 130.3, 128.9, 127.9, 127.2, 118.2, 57.0, 25.4, 23.3, 9.3; HRMS-ESI (m/z) Calcd. $C_{22}H_{22}ON_3Cl_3$ + H)+: 463.0854 found:463.0853.

N′-(5-(4-chlorophenyl)-1-(2,4-dichlorophenyl)-4-methyl-1H-pyrazole-3-carbonyl) isonicotinohydrazide (**4**) Compound **4** was synthesized according to the procedure applied to **1**. Off white solid: 499 mg, 59 %; mp 237–239 °C; ^{1}H NMR ($CDCl_3$, 400 MHz): δ 10.33 (s,1H), 9.44 (s, 1H), 8.71 (s, 1H), 7.74 (s, 2H), 7.41 (s, 1H), 7.30–7.32 (m, 5H), 7.05 (d, $J = 8.53$ Hz, 2H), 2.17 (s, 3H); ^{13}C NMR ($CDCl_3$, 100 MHz): δ 163.5, 161.2, 150.2, 143.3, 142.4, 136.2, 135.6, 135.2, 132.7, 130.7, 130.5, 130.3, 128.9, 128.8, 127.9, 126.7, 118.4, 30.9, 9.2; HRMS-ESI (m/z) $C_{23}H_{16}O_2N_5Cl_3$ + H)+: Calcd. 500.0442 found: 500.0443.

(5-(4-chlorophenyl)-1-(2,4-dichlorophenyl)-4-methyl-1H-pyrazol-3-yl)(4-methylpiperazin-1-yl) methanone (**5**) Compound **5** was synthesized according to the procedure applied to **1**. Brown solid; 306 mg, 50 %; mp 111–113 °C;

^{1}H NMR ($CDCl_3$, 400 MHz): δ 7.48 (s, 1H), 7.31–7.34 (m, 3H), 7.20 (d, J = 8.54 Hz, 1H), 7.10 (d, J = 8.28 Hz, 2H), 3.99–3.80 (m, 4H), 2.61–2.45 (m, 4H), 2.37 (s, 3H), 2.24 (s, 3H); ^{13}C NMR ($CDCl_3$, 100 MHz): δ 163.2, 146.4, 141.9, 135.9, 135.7, 134.8, 133.0, 130.6, 128.9, 127.8, 127.3, 116.8, 55.5, 54.7, 47.1, 45.9, 41.9, 9.0; HRMS-ESI (m/z) $C_{22}H_{21}ON_4Cl_3$ + H) + :Calcd. 463.0854 found: 463.0862.

(5-(4-chlorophenyl)-1-(2,4-dichlorophenyl)-4-methyl-1H-pyrazol-3-yl) (morpholino) methanone (**6**) Compound **6** was synthesized according to the procedure applied to **1**. Cream yellow solid: 590 mg, 63 %; mp 170–172 °C;^{1}H NMR ($CDCl_3$, 500 MHz): δ 7.47 (d, J = 2 Hz, 1H), 7.33 (d, J = 8.54 Hz, 2H), 7.27–7.30 (m, 1H), 7.19 (d, J = 8.55 Hz, 1H), 7.09 (d, J = 8.54 Hz, 2H), 3.85–3.92 (m, 4H), 3.75–3.83 (m, 4H), 2.25 (s, 3H); ^{13}C NMR ($CDCl_3$, 125 MHz): δ 163.2, 146.0, 142.1, 135.9, 135.8, 134.9, 133.0, 130.6, 130.5, 130.3, 128.9, 127.8, 127.3, 117.2, 67.3, 66.9, 47.8, 42.6, 9.1; HRMS-ESI (m/z) $C_{21}H_{18}O_2N_3Cl_3Na$:Calcd. 472.0357 found: 472.0355.

N′-(1-(2,4-dichlorophenyl)-4-methyl-5-phenyl-1H-pyrazole-3-carbonyl)isonicotinohydrazide (**10**) Compound **10** was synthesized according to the procedure applied to **1**. White solid: 273 mg, 68 %; mp 167–168 °C; ^{1}H NMR ($CDCl_3$, 400 MHz): δ 10.28 (bs, 1H), 9.43 (s, 1H), 8.71 (bs, 1H), 7.75 (s, 1H), 7.41 (d, J = 1.47, 2H), 7.28–7.34 (m, 5H), 7.14 (d, J = 4.40, 2H), 7.01–7.04 (m, 1H) 2.33 (s,3H); ^{13}C NMR ($CDCl_3$, 100 MHz): δ 163.4, 161.2, 150.3, 144.4, 142.3, 138.8, 135.9, 135.8, 132.8, 130.5, 130.2, 129.5, 128.9, 128.6, 128.2, 127.8, 121.2, 118.3, 9.3; HRMS-ESI (m/z) $C_{23}H_{17}O_2N_5Cl_2$ + H)+: Calcd. 466.0832 found: 463.0830.

5-(4-chlorophenyl)-4-methyl-1-phenyl-N-(piperidin-1-yl)-1H-pyrazole-3-carboxamide (**14**) Compound **14** was synthesized according to the procedure applied to **1**. White solid; 580 mg, 65 %; mp 201–202 °C; ^{1}H NMR ($CDCl_3$, 400 MHz): δ 7.77 (bs, 1H), 7.33 (d, J = 7.27 Hz, 5H), 7.21 (d, J = 7.78 Hz, 2H), 7.08 (d, J = 8.28 Hz, 2H), 2.98–2.79 (m, 4H), 2.35 (s, 3H), 1.85–1.68 (m, 4H), 1.52–1.38 (m, 2H); ^{13}C NMR ($CDCl_3$, 100 MHz): δ 160.1, 143.5, 140.9, 139.3, 134.6, 131.2, 129.0, 128.9, 128.0, 127.9, 125.0, 119.1, 57.1, 25.4, 23.3, 9.3; HRMS-ESI (m/z) $C_{22}H_{23}ON_4Cl$ + H)$^+$: Calcd. 395.1633 found: 395.1631.

1-(2-chlorophenyl)-5-(4-chlorophenyl)-4-methyl-N-(piperidin-1-yl)-1H-pyrazole-3-carboxamide (**15**) Compound **15** was synthesized according to the procedure applied to **1**. Yellow solid: 207 mg, 42 %; mp 248–250 °C; ^{1}H NMR ($CDCl_3$, 200 MHz): δ 7.69 (bs, 1H), 7.37–7.30 (m, 1H),7.29–7.24 (m, 2H), 7.23–7.15 (m, 3H), 6.98 (d, J = 8.71 Hz, 2H), 2.95–2.72 (m, 4H), 2.30 (s,3H), 1.78–1.61 (m, 4H), 1.45–1.29 (m, 2H); ^{13}C NMR ($CDCl_3$, 100 MHz): δ 160.3, 143.4, 141.1, 136.5, 135.0, 131.5, 130.9, 130.8, 130.3, 129.8, 128.8, 127.7, 126.6, 118.3, 55.7, 23.8, 21.1, 9.2; HRMS-ESI (m/z) $C_{22}H_{22}ON_4Cl_2$ + H)$^+$: Calcd. 429.1243 found: 429.1246.

(5-(4-chlorophenyl)-1-(2,4-difluorophenyl)-4-methyl-1H-pyrazol-3-yl)(4-methylpiperazin-1-yl) methanone (**16**) Compound **16** was synthesized according to the procedure applied to **1**. White solid; 518 mg, 84 %; mp 174–176 °C; ^{1}H NMR ($CDCl_3$, 200 MHz): δ 7.30–7.24 (m, 1H), 7.24–7.20 (m, 2H), 7.06–6.96 (m, 2H), 6.91–6.69 (m, 2H), 3.91–3.63 (m, 4H), 2.56–2.34 (m, 4H), 2.29 (s, 3H), 2.12 (s, 3H); ^{13}C NMR ($CDCl_3$, 50 MHz): δ 163.2, 146.6, 141.9, 134.8, 130.5, 129.7, 128.8, 127.4, 124.1, 116.8, 112.1, 111.6, 105.0, 104.5, 55.5, 54.7, 47.0, 45.9, 41.8, 8.9; HRMS-ESI (m/z) $C_{22}H_{21}ON_4ClF_2$ + H)$^+$: Calcd. 431.1445 found: 431.1447.

5-(4-chlorophenyl)-4-methyl-N-(piperidin-1-yl) isoxazole-3-carboxamide (**17**) Compound **17** was synthesized according to the procedure applied to 1. White solid: 240 mg, 45 %; mp 103–104 °C; ^{1}H NMR ($CDCl_3$, 500 MHz): δ 7.63–7.64 (d, J = 8.24 Hz, 1H), 7.57–7.58 (d, J = 8.24 Hz, 1H), 7.47–7.49 (d, J = 8.24 Hz, 2H), 2.99–2.81 (m, 4H), 2.45 (s, 3H), 1.85–1.71 (m, 4H), 1.53–1.41 (m, 2H); ^{13}C NMR ($CDCl_3$, 125 MHz): δ 165.8, 163.0, 157.3, 156.4, 136.1, 129.2, 126.0, 111.7, 56.9, 25.2, 23.1, 8.3; HRMS-ESI (m/z) $C_{16}H_{18}O_2N_3Cl$ + H)$^+$: Calcd. 320.1160 found: 320.1161.

1-(2,4-dichlorophenyl)-4-methyl-5-phenyl-N-(piperidin-1-yl)-1H-pyrazole-3-carboxamide (**18**) Compound **18** was synthesized according to the procedure applied to **1**. Pale brown solid: 288 mg, 61 %; mp 172–173 °C; ^{1}H NMR ($CDCl_3$, 400 MHz): δ 7.72 (s, 1H), 7.41 (s, 1H), 7.27–7.32 (m, 5H), 7.11 (s, 2H), 3.05–2.75 (m, 4H), 2.38 (s, 3H), 1.91–1.65 (m, 4H), 1.54–1.34 (m, 2H); ^{13}C NMR ($CDCl_3$, 100 MHz): δ 160.1, 144.2, 144.0, 136.1, 135.7, 133.0, 130.6, 130.2, 129.5, 128.6, 128.6, 128.4, 127.7, 117.9, 57.0, 25.3, 23.2, 9.3; HRMS-ESI (m/z) $C_{22}H_{22}ON_4Cl_2$ + H)$^+$: Calcd. 429.1243 found: 429.1244.

5-(4-chlorophenyl)-1-(2,4-dichlorophenyl)-N-(piperidin-1-yl)-1H-pyrazole-3-carboxamide (**19**) Compound **19** was synthesized from the corresponding acid according to the procedure applied to **1**. Cream solid: 199 mg, 53 %; mp 139–140 °C; ^{1}H NMR ($CDCl_3$, 400 MHz): δ 7.61 (d, J = 2.29 Hz, 1H), 7.57 (s, 1H), 7.55 (d, J = 2.29 Hz, 1H), 7.53 (d, J = 1.83 Hz, 1H), 7.42 (d, J = 9.15 Hz, 2H), 7.26 (d, 2H), 7.23 (s, 1H), 3.35–3.19 (m, 4H), 2.01–1.95 (m, 4H), 1.70–1.59 (m, 2H); ^{13}C NMR ($CDCl_3$, 100 MHz): δ 158.8, 146.8, 145.6, 136.3, 135.7, 135.1, 132.8, 130.5, 130.4, 129.1, 129.0, 128.2, 127.3, 107.5, 56.8, 24.9, 22.7; HRMS-ESI (m/z) $C_{21}H_{19}ON_4Cl_3$ + H)$^+$: Calcd. 449.0697 found: 449.0701.

Anti-mycobacterial activity assay (Abreu *et al*., 2012; Stigliani *et al*., 2012; Handoko *et al*., 2012; Tiwari *et al*., 2012; NCCLS, 1995)

Isolated single colonies of *M. smegmatis* MC2155 (ATCC 14468) grown on 7H10 agar plate were developed overnight in Middlebrook 7H9 medium (0.47 % Middlebrook 7H9 broth base, 10 % ADS, 0.2 % glycerol and 0.1 % Tween 80) to mid-exponential phase at 37 °C. When the OD of this culture reached approximately 0.8, a secondary culture was inoculated in 5 ml Middlebrook 7H9 medium. The secondary culture was incubated overnight and allowed to grow at 37 °C to early log phase (OD600 $\approx$ 0.3). For the anti-mycobacterial assay, 98 µl of 1:1000-folds dilution of the secondary culture was dispensed into 96-well microtiter plate per well along with 2 µl of test compound in triplicate, and 240 µl of sterile water was added to each well of the peripheral rows of 96-well plate to minimize media evaporation during assay incubation. The final concentration of the test compound in each well was 30 µM. Bacterial growth was assessed after 32 h of incubation by measuring turbidity at 600 nm OD600 values using TECAN Infinite 200 PRO^{TM} (Tecan Instruments, Switzerland). Depending upon the percentage of growth, the percentage of inhibition was calculated at a standard concentration of 30 µM. Isoniazid and rifampicin were included in every assay plate as positive controls of growth inhibition using stock solutions of INH (10 mg/ml, HiMedia) and rifampicin (10 mg/ml, HiMedia) to achieve the final concentration of 16 µg/ml for INH and 2 µg/ml for rifampicin. Additional controls DMSO (solvent without compound) and medium without inoculums were included in all the assay plates avoiding intra-assay variability. The results were analyzed as the percentage of growth inhibition.

MIC Assay (Abreu *et al*., 2012; Stigliani *et al*., 2012; Handoko *et al*., 2012; Tiwari *et al*., 2012; NCCLS, 1995)

After the compounds were screened for percentage inhibition, the promising compounds were further screened to obtain the MIC values. Minimum inhibitory concentration (MIC) is the concentration of compound which inhibits the 90 % growth of bacteria under optimum conditions. The growth inhibition assays were carried out in the same analogy as explained above using various concentrations of the test compounds prepared by serial dilutions 100, 50, 25, 12.5 and 6.25 µM to obtain the final concentrations of 46.37, 23.18, 11.59, 5.79 and 2.89 µg/ml, respectively. From the rate of inhibition bacterial growth, the ascertained MIC of the compound was calculated. The MIC value of the test compound 1 (rimonabant) is 13.56 µg/ml (29.24 µM $\pm$ 1.47).

In vitro anti-mycobacterial activity against *M. tuberculosis* H37Rv (MTB) (Abreu *et al*., 2012; Stigliani *et al*., 2012; Handoko *et al*., 2012; Tiwari *et al*., 2012; NCCLS, 1995).

MTB H37Rv strain was obtained from National Institute for Research in Tuberculosis (NIRT), Chennai. Tenfold serial dilutions of each test compound were prepared and incorporated into Middlebrook 7H11 agar medium with OADC growth supplement. Inoculation of *M. tuberculosis* H37Rv ATCC 27294 (MTB) was prepared from fresh Middlebrook 7H11 slants with OADC growth supplement and was adjusted to 1 mg/ml (wet weight) in Tween 80 (0.05 %) saline diluted to 10–2 to achieve a concentration of $\sim$107 cfu/ml (culture forming units). Then, a bacterial suspension of 5 µl was spotted in 7H11 agar tubes having tenfold serial dilutions of compounds per ml. Cultures were then incubated at 37 °C for 4 weeks. The MIC values of the synthesized compounds along with the standard drugs for comparison are tabulated in Table 1.

Experimental methodology for molecular docking analysis

For molecular docking, the structures were drawn using ChemDraw 12 followed by MMFF94 optimization using the default settings. The crystallographic coordinates of CYP121 (pdb id: 2IJ7) from *M. tuberculosis* were obtained from protein data bank (www.rcsb.org). For CYP121 of *M. tuberculosis*, we opted for pdb-2IJ7 for docking, because it has been crystallized with fairly good resolution (1.90 Å) with fluconazole as a ligand. For docking analysis, the standard procedure mentioned in literature (Abreu *et al*., 2012; Stigliani *et al*., 2012; Handoko *et al*., 2012; Tiwari *et al*., 2012; Masand *et al*., 2013) was followed using AutoDock 4.2, running under Linux Ubuntu 12.04.

Acknowledgments JMG gratefully acknowledges CSIR-OSDD, CSIR-ORIGIN and DST-SERB, for the financial support.

References

Abreu RM, Froufe HJ, Queiroz MJ, Ferreira IC (2012) Selective flexibility of side-chain residues improves VEGFR-2 docking score using AutoDock Vina. Chem Biol Drug Des 79(4):530–534

Belin P, Le Du MH, Fielding A, Lequin O, Jacquet M, Charbonnier JB, Lecoq A, Thai R, Courcon M, Masson C, Dugavet R, Pernodet JL, Gondry M (2009) Identification and structural basis of the reaction catalyzed by CYP121, an essential cytochrome P450 in *Mycobacterium tuberculosis*. Proc Natl Acad Sci USA 106(18):7426–7431

Chiang CY, Schaaf HS (2010) Management of drug-resistant tuberculosis. Int J Tuberc LungDis 14:672–682

Corbett EL, Watt CJ, Walker N, Maher D, Williams BG, Raviglione MC, Dye C (2003) The growing burden of tuberculosis: global

trends and interactions with the HIV epidemic. Arch Intern Med 163(9):1009–1021

Dumas VG, Defelipe LA, Petruk AA, Turjanski AG, Marti MA (2013) QM/MM study of the C–C coupling reaction mechanism of CYP121, an essential cytochrome p450 of mycobacterium tuberculosis. Proteins 82(6):1004–1021

Elzinga G, Raviglione MC, Maher D (2004) Scale up: meeting targets in global tuberculosis control. Lancet 363(9411):814–819

Handoko SD, Ouyang X, Su CT, Kwoh CK, Ong YS (2012) QuickVina: accelerating AutoDock Vina using gradient-based heuristics for global optimization. IEEE/ACM Trans Comput Biol Bioinform. 9(5):1266–1272

Hudson SA, McLean KJ, Surade S, Yang Y-Q, Leys D, Ciulli A, Munro AW, Abell C (2012) Application of fragment screening and merging to the discovery of inhibitors of the mycobacterium tuberculosis cytochrome P450 CYP121. Angew Chem Int Ed 51(37):9311–9316

Jagerovic N, Fernandez-Fernandez C, Goya P (2008) CB1 cannabinoid antagonists: structure-activity relationships and potential therapeutic applications. Curr Top Med Chem 8(3):205–230

Kang JG, Park CY (2012) Anti-obesity drugs: a review about their effects and safety. Diabetes Metab J 36(1):13–25

Kotagiri VK, Suthrapu S, Mukunda Reddy J, Prasad Rao C, Bollugoddu V, Bhattacharya A, Bandichor R (2007) An improved synthesis of rimonabant: anti-obesity drug. Org Proc Res Dev 11:910–912

Kumar V, Kaur K, Gupta GK, Sharma AK (2013) Pyrazole containing natural products: synthetic preview and biological significance. Eur J Med Chem 69:735–753

Lan R, Liu Q, Fan P, Lin S, Fernando SR, McCallion D, Pertwee R, Makriyannis A (1999) Structure-activity relationships of pyrazole derivatives as cannabinoid receptor antagonists. J Med Chem 42(4):769–776

Lange JH, Kruse CG (2005) Keynote review: medicinal chemistry strategies to CB1 cannabinoid receptor antagonists. Drug Discov Today 10(10):693–702

Masand VH, Jawarkar RD, Mahajan DT, Hadda TB, Sheikh J, Patil KN (2012) QSAR and CoMFA studies of biphenyl analogs of the anti-tuberculosis drug (6S)-2-nitro-6-{[4-(trifluoromethoxy) benzyl]oxy}-6,7-dihydro-5H-imidazo[2,1-b][1,3]oxazine(PA-824). Med Chem Res 21:2624–2629

Masand VH, Mahajan DT, Hadda TB, Jawarkar RD, Chavan H, Bandgar BP, Chauhan H (2013) Molecular docking and quantitative structure–activity relationship (QSAR) analyses of indolylarylsulfones as HIV-1 non-nucleoside reverse transcriptase inhibitors. Med Chem Res 23(1):417–425

McLean KJ, Marshall KR, Richmond A, Hunter IS, Fowler K, Kieser T, Gurcha SS, Besra GS, Munro AW (2002) Azole antifungals are potent inhibitors of cytochrome P450 mono-oxygenases and bacterial growth in mycobacteria and streptomycetes. Microbiology 148:2937–2949

Menozzi G, Merello L, Fossa P, Schenone S, Ranise A, Mosti L, Bondavalli F, Loddo R, Murgioni C, Mascia V, La Colla P, Tamburini E (2004) Synthesis, antimicrobial activity and molecular modeling studies of halogenated 4-[1H-imidazol-1-yl(phenyl)methyl]-1,5-diphenyl-1H-pyrazoles. Bioorg Med Chem 12(20):5465–5483

Moore AV, Kirk SM, Callister SM, Mazurek GH, Schell RF (1999) Safe determination of susceptibility of Mycobacterium tuberculosis to antimycobacterial agents by flow cytometry. J. Clin Microbio 37(3):479–483

NCCLS-National Committee for Clinical Laboratory Standards (1995) Antimycobacterial susceptibility testing for Mycobacterium tuberculosis proposed standard M24-T. Villanova, PA

Nunn P, Williams B, Floyd K, Dye C, Elzinga G, Raviglione M (2005) Tuberculosis control in the era of HIV. Nature Rev Immunol 5(10):819–826

Shukla D, Mesfin YM, Hailemariam D, Biadglign S, Kibret KT (2014) Association between HIV/AIDS and multi-drug resistance tuberculosis: a systematic review and meta-analysis. PLoS ONE 9(1):e82235

Stigliani JL, Bernardes-Genisson V, Bernadou J, Pratviel G (2012) Cross-docking study on InhA inhibitors: a combination of Autodock Vina and PM6-DH2 simulations to retrieve bio-active conformations. Org Bio-Mol Chem 10(31):6341–6349

Sundaramurthi JC, Kumar S, Silambuchelvi K, Hanna LE (2011) Molecular docking of azole drugs and their analogs on CYP121 of mycobacterium tuberculosis. Bioinformation 7(3):130–133

Tiwari A, Saxena S, Pant AB, Srivastava P (2012) Protein-ligand interaction studies of retinol-binding protein 3 with herbal molecules using AutoDock for the management of Eales' disease. J Ocul Biol Dis Infor 5(2):40–43

www.who.int/topics/tuberculosis/en/, Global Tuberculosis Report 2013, in, 2013

www.who.int/topics/tuberculosis/en/, Tuberculosis prevalence surveys: a handbook, in, 2011